JOURNAL OF SOLID STATE CHEMISTRY 51, 1–16 (1984)

Electrolytic Coloration and Electrical Breakdown of MgO Single Crystals*

M. M. ABRAHAM, L. A. BOATNER, W. H. CHRISTIE,† AND F. A. MODINE.

Solid State Division, Oak Ridge National Laboratory, Oak Ridge, Tennessee 37830

T. NEGAS

National Bureau of Standards, Washington, D.C. 20234

AND R. M. BUNCH‡ AND W. P. UNRUH

Department of Physics, University of Kansas, Lawrence, Kansas 66044

Received April 22; in revised form July 1, 1983

A series of investigations of electrolytic coloration effects produced in MgO single crystals containing iron-group impurities has been carried out. The purpose of these investigations was to determine the identity and production mechanism of localized coloration or dark streaks that are frequently observed following the electrical breakdown of MgO crystals at temperatures in the range of 1000°C. A technique employing a point contact cathode was used to reproduce these coloration effects in a controlled systematic manner. Studies using a variety of techniques (MCD, EPR, SIMS, light scattering, etc.) establish that the formation of metallic precipitates by electrolytic reduction of impurities is primarily responsible for the observed localized dark coloration effects. *In situ* observations of the coloration process showed that it was initiated at the cathode and that the regions of coloration are coincident with those regions of the MgO crystal where the catastrophic failure in electrical insulating properties occurs. Electrical breakdown and coloration effects were observed in MgO crystals doped with each member of the entire 3*d* transition series except scandium. Crystals doped with different impurities did vary, however, in their tendency to fail electrically. Similar solid state chemical alterations were induced by more conventional reduction techniques which generally required higher temperatures to produce metallic colloids than electrolysis.

I. Introduction

While magnesium oxide is regarded as one of the better electrical insulators in the general class of refractory oxide materials, there are reports (*1*, *2*) of catastrophic electrical failure in MgO single crystals that were subjected to moderate electric fields (~1000 V/cm) and temperatures (~1000°C) for time periods of ≥100 hr. This reported catastrophic electrical failure was characterized by a rapid increase in electrical conductivity of the single-crystal sample. An effect of this type obviously has serious implications regarding the practical long-term

*Research sponsored by the Division of Materials Sciences, Office of Basic Energy Sciences, U.S. Department of Energy, under Contract W-7405-eng-26 with Union Carbide Corporation.

† Analytical Chemistry Division, ORNL.

‡ Present address: San Diego State University, San Diego, Calif. 92182.

0022-4596/84 $3.00

utility of MgO as an insulator at elevated temperatures. In most of the MgO crystals for which thermal-electrical breakdown was reported in Ref. (*1*), darkened regions were observed which extended either completely or partially across the specimen between the electrodes. Transmission electron microscopy was used in an examination of these dark regions or "streaks" and a new type of defect (dislocation loops with a ⟨100⟩ Burgers vectors lying in {100} planes) was reported (*2*). As noted in Ref. (*1*), however, the results reported by Narayan *et al.* (*2*) show that "there is *no* evidence for metal-precipitate formation either of impurities or of Mg." While a possible relationship between the failure in the high temperature electrical insulating properties of MgO and the observed dislocation loops was suggested by Sonder *et al.* (*1*), neither the cause of this "thermal-electrical" breakdown nor the nature of the dark streaks observed following breakdown was established.

The present work summarizes a series of investigations (*3–5*) carried out to establish the identity and production mechanism for the dark "streaks" that accompany most cases of electrical breakdown in MgO at elevated temperatures. The thermal-electrical breakdown and dark "streak" development were studied as a function of impurity content, and analytical and spectroscopic techniques were used in determining the composition of the colored areas comprising the streaks. The results of these investigations establish that (i) the dark coloration found in MgO following electrical breakdown at elevated temperatures is either entirely or largely due to the presence of metallic precipitates; (ii) the metallic precipitates are produced by an electrolytic reduction of impurities; (iii) the colored regions of the MgO single crystals coincide with the regions of high electrical conductivity; (iv) the electrolytic coloration originates at the cathode and eventually progresses to the anode; (v) a reversal in the polarity of the applied E field can produce a clearing up of previously darkened areas. While this effect was not investigated in detail, it was possible to clear approximately 50% of the coloration in several samples containing different ion group impurities by E-field reversal. No attempts were made to clear the entire coloration by prolonged treatments, and (vi) similar coloration effects associated with the formation of metallic precipitates can be produced by standard reduction techniques other than electrolytic treatments (e.g., by simply reducing doped MgO crystals in a hydrogen atmosphere at high temperatures, i.e., >1200°C).

II. Experimental

Initial studies of the colored regions associated with "thermal-electrical" breakdown of MgO were performed using two single-crystal samples with unknown impurity content that were supplied by Sonder *et al.* (*1*). These samples consisted of small (~2 mm^3), darkly colored pieces cut from larger MgO crystals (Norton Co.) that had failed electrically after a relatively long period of time (≥100 hr) in the apparatus described in Ref. (*1*). Subsequently, samples containing a well-defined colored region whose origin was controlled were prepared by a method similar to a technique used previously to produce electrolytic coloration in alkali halides (*6*). A diagram of the associated apparatus is shown in Fig. 1a along with a photograph (see Fig. 1c) of a single region of dark coloration produced in a manganese-doped MgO crystal. As shown in Fig. 1a, a pointed platinum, single-contact cathode was used; and the associated high E field resulted both in the rapid formation of a dark "streak" and in electrical breakdown at temperatures of about 1050°C. These effects could often be produced in 2 hr or less as compared to the

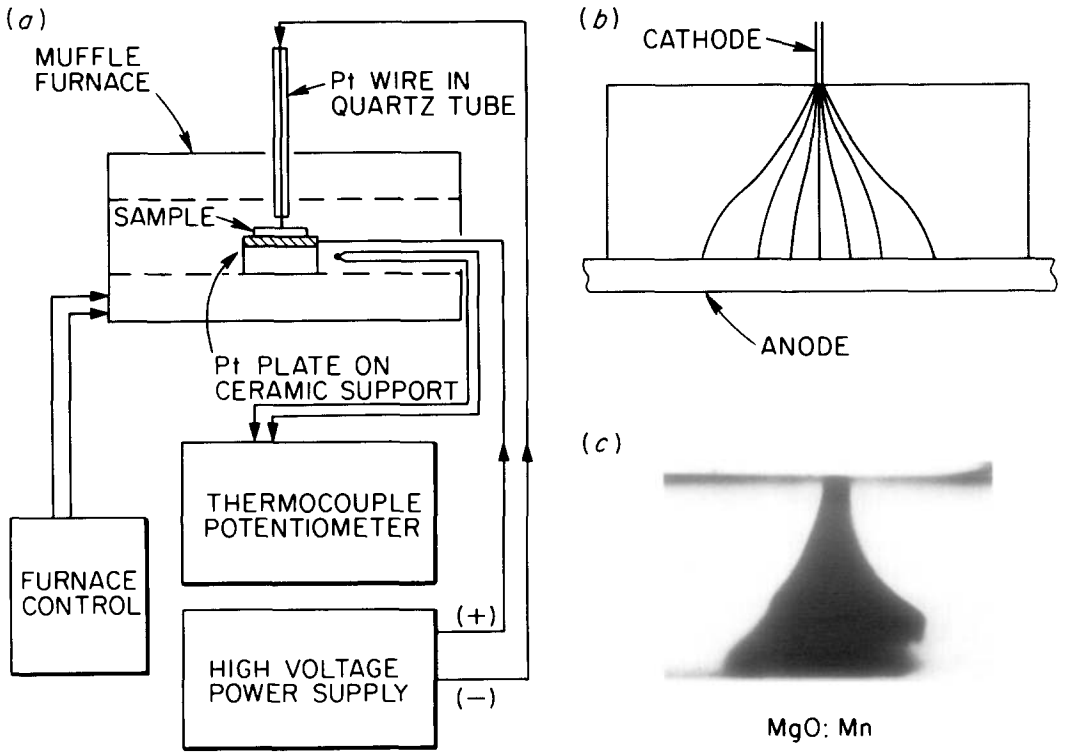

FIG. 1. Schematic diagram of the electrolytic coloration apparatus and the *E*-field lines in a planar dielectric along with a photograph of an electrolytically colored area in an MgO crystal. (a) Apparatus permitting the direct visual observation of the development of colored streaks; (b) a sketch of the sample and electrode configuration showing a qualitative representation of the electric-field flux lines present in the sample; (c) photograph of an MgO : Mn crystal following a treatment at 1050°C and an applied voltage of 1100 V for 2 hr. Note the similarity between the shape of the altered region and the *E*-field distribution in the sample.

~100-hr time periods characteristic of the technique described in Ref. (*1*) where planar platinum electrodes were employed. Additionally, the apparatus shown schematically in Fig. 1a was configured in a manner that permitted direct observations of the initiation and growth of the dark streaks to be made by means of a telescope. This apparatus was used in preparing numerous samples of selectively colored MgO crystals that differed principally in their content (both type and amount) of 3*d* transition metal impurities. The MgO single crystals that were electrolytically treated in this apparatus were either grown at ORNL (*7*) or were purchased from the Norton Company. The specimens typically had dimensions of 1 × 1 × 0.25 cm. Optical properties of the colored and "clear" regions of the samples were determined from absorption spectra obtained with a Cary-14 spectrophotometer and from Mie scattering (*8*) studies performed using a He–Ne laser. Magnetic properties of the colored streaks were studied by electron paramagnetic resonance and magneto-optical techniques. Magnetic resonance spectra were obtained at room temperature and at 77 K using both *X*-band and *K*-band homodyne spectrometers. Magnetic circular dichroism (MCD) (*9*) spectra were used to relate directly the dark coloration to ferromagnetic impuri-

ties. (MCD is simply the magnetically induced difference between the absorption of left and right circularly polarized light.) The composition of the dark streaks was determined by chemical analysis, secondary ion mass spectroscopy (SIMS), and X-ray fluorescence spectroscopy (XFS). The SIMS measurements utilized an oxygen ion beam.

III. Electrolytic Coloration

While the two original Norton samples provided by Sonder *et al.* (*1*) were used in establishing that the dark streaks in these particular crystals were due to ferromagnetic particles, the systematic study of electrolytic coloration was carried out using samples treated with the apparatus shown in Fig. 1. Undoped MgO crystals and MgO samples intentionally doped with various iron-group impurities were electrolytically treated at ~1050°C for various time periods. Table I lists some of the applied voltages, time periods, and samples that were treated; it also includes comments on the changes induced in the crystals. The dopants listed in Table I represent the predominant impurity (typically on the order of several hundred parts per million). Many of the samples, however, contained Fe, Al, Ca, and Si at concentrations of between 10 and a few hundred ppm. A few parts per million of other iron group impurities such as Mn and Cr and trace amounts of other elements were also present. Even the purest samples contained between 1 and 10 ppm Fe. Although a precise classification of the effect of a particular impurity is not possible because several impurities were always present, the connection between the impurities, electrolytic coloration, and electrical

TABLE I

CONDITIONS AND RESULTS OF ELECTROLYTIC TREATMENTS

Crystal	Temperature (°C)	Applied voltage (V)	Time (hr)	Result
MgO : Fe	1050	1800	42	Single well-defined dark streak, general clearing of original pale yellow color
MgO : Mn	1050	1100	2	Dense well-defined cone-shaped streak
MgO : Mn	1050	1200	96	Extensive coloration
MgO : Co	1050	1500	2	Dark coloration near the cathode surrounded by a diffuse ring
MgO : Co	1050	750	45	Complete dark coloration of the entire crystal
MgO : V	1050	1400	3	Brown streak surrounded by a clear area inside a purple ring
MgO : V	1050	950	19	Broad streaks surrounded by clear areas
MgO : Cr	1050	1000	45	Coloration over 50% of the sample volume
MgO : Cr	1050	1000, 1200	25, 19	Broad extensive coloration
MgO : Ni	1050	1500	11	Broad diffuse coloration
MgO : Ni	1050	1500	24	Extensive dark coloration
MgO : Cu	1050	1200	97	Dark streak and diffuse coloration
MgO : Li	1050	1200	22	Conducting, but no coloration
MgO (pure)	1050	1700	18	Faint coloration located along crack
MgO (purest)	1050	1240	45	No coloration
MgO (purest)	1050	1700, 2500	18, 45	Sample cracked, but no coloration
NaCl : Cu	450	200	18	Dense extensive coloration; electrical breakdown observed in <30 min

breakdown was clearly established. Electrolytic treatments produced dark streaks in all of the specimens containing significant concentrations of 3*d* transition metal impurities; visible coloration was not produced in the purest specimens even though electrical breakdown occurred. An impurity-related difference in the tendency toward breakdown was observed, however. Examples of the electrolytic coloration effects observed in MgO single crystals doped with four different iron-group impurities are shown in Figs. 2a, b, c, and 3a, b. Figure 2a shows a cross-sectional view (i.e., in a direction parallel to the 1.0 × 1.0-cm major faces) of a manganese-doped MgO sample treated at 1050°C for 2 hr with an 1100-V potential applied between the point contact and planar platinum electrodes. The narrow top portion of the "conical," "volcano-shaped" dark region of the crystal is located at the position where the cathode point contact was made. Near the broad bottom of the cone where the coloration has not proceeded to the point of making the entire area completely opaque, the altered portion of the crystal is apparently a dark brownish, amber color.

Figure 2b shows a cross-sectional view of an iron-doped MgO crystal that was treated for 42 hr at 1050°C. Prior to the electrolytic treatment, the entire crystal was uniformly yellow in color. This color has been bleached from the top (cathode) portion of the crystal shown in Fig. 2b but is still present to some extent in a nonuniform layer on the bottom side that was adjacent to the planar platinum anode in the treatment furnace. The crystal has a small "check" or crack at the point of application of the pointed cathode, and the single, well-defined dark streak emanates from the bottom portion of this crack and extends across the remainder of the specimen. Electrolytic treatments that were carried out for extended time periods often produced cracks of this type at the point-contact cathode. One significant observation that can be made from the results obtained for Fe-doped MgO is that while solid state chemical changes occur throughout the entire volume of the crystal, as evidenced by the complete change of color from yellow to clear that results from extended treatments, the conditions leading to the formation of the extensively altered "dark streaks" appear to be associated with the regions of the highest *E* fields. The *E*-field distribution associated with an electrode configuration of the type employed here is shown schematically in Fig. 1b. A comparison of the relatively narrow streak produced in the MgO:Fe sample or the more extensive streak shown in Fig. 2a for MgO:Mn with the field distribution shown in Fig. 1b shows a close correspondence between the *E*-field distribution and the shape of the heavily altered portion of the crystal.

While the formation of simple, well-defined streaks similar to those shown in Figs. 2a and 2b was observed in some MgO-iron-group impurity systems, in MgO crystals doped with other iron group impurities more complex solid state chemical alterations were in evidence. Examples of such effects are given in Fig. 2c and Figs. 3a,b. Figure 2c shows the effects observed in a single crystal of MgO doped with vanadium. The view in this illustration is normal to the top (~1 × 1 cm) broad face of the sample, i.e., the view is parallel to the platinum wire that terminated in the point contact. In this example, the point contact was moved to an adjacent position on the crystal face after 1.5 hr and, accordingly, two altered regions were produced in the course of the 3-hr electrolytic treatment at 1400 V and 1050°C. In this case, the altered portions consist of a series of concentric, cylindrical sections (with the axis of the cylinder parallel to the point contact wire). Both altered regions in Fig. 2c extended completely across the narrow dimension of the

sample. The central portion of the altered area (i.e., the area coincident with the point contact) is characterized by a brownish, amber color, as shown in Fig. 2c. This "streak" is surrounded by a clear cylindrical region which, in turn, is surrounded by a cylindrical shell characterized by a dark violet color. This structure, which is distributed in the same manner as the rings of a tree about the centroid of the point contact, illustrates the different redox conditions present in the sample as a function of distance from the cathode.

An additional example of complex electrolytic effects produced in a doped MgO single crystal is shown in Figs. 3a,b. In this illustration a top view and a cross-sectional view of an MgO:Co specimen treated for 2 hr at 1050°C and with an applied voltage of 1500 V are shown. The original color of the sample can still be seen at the crystal corners and outside edges. An area of dense coloration was formed that originates at the cathode, but this region did not completely traverse the sample (from cathode to anode) during the 2-hr duration of the electrolytic treatment. Instead, an extensive diffuse ring of amber coloration was produced across the entire thickness of the crystal.

Additional electrolytic coloration phenomena that were observed in various MgO-impurity systems are noted in Table I. In each case where a dark streak was formed, the streak always progressed from the cathode to the anode, and was eventually accompanied by a large increase in the conductivity of the sample. The voltage from the high impedence (100 kΩ) power supply dropped abruptly at breakdown even though a 100-kΩ resistor was placed in series with the sample to limit the breakdown current. Prior to the electrical breakdown, virtually all of the voltage was dropped across the approximately 100-MΩ resistance of the sample. It was confirmed that the high conductivity associated with electrical breakdown was confined to the immediate vicinity of the streak (i.e., the area of the streak itself was conducting) by simply moving the point contact to a new location. This movement reduced the current to prebreakdown levels until a new streak formed and a second breakdown occurred.

The time required to produce electrolytic coloration and breakdown in MgO decreases as the temperature and voltage increase. Differences were noticed in the ease with which samples containing different impurity concentrations would color and break down. The samples doped with V, Mn, Co, and Ni colored most readily, while those containing Cr and Fe appeared to be more difficult to color and break down. Conclusions regarding a Cu dopant are uncertain because this impurity was present in relatively low concentrations (~100 ppm) in the available samples. Magnesium oxide doped with lithium was also investigated. The atypical behavior of this material may be due to the fact that MgO:Li initially has an inherently high conductivity. Additionally, sodium chloride doped with copper was treated and has been listed in Table I to emphasize that similar phenomena are observed in the alkali halides at lower voltages and temperatures. Electrolytically colored regions whose properties were either qualitatively described above or listed in Table I have been investigated using a variety of characterization techniques. The solid state chemical and physical characteristics determined as a result of these studies are discussed in the following sections.

IV. Optical Studies

Since many of the colored areas of electrolytically treated doped MgO crystals were either nearly opaque or very inhomogeneously colored, the optical studies were difficult. Accordingly, the quantitative aspects of the optical spectra are not com-

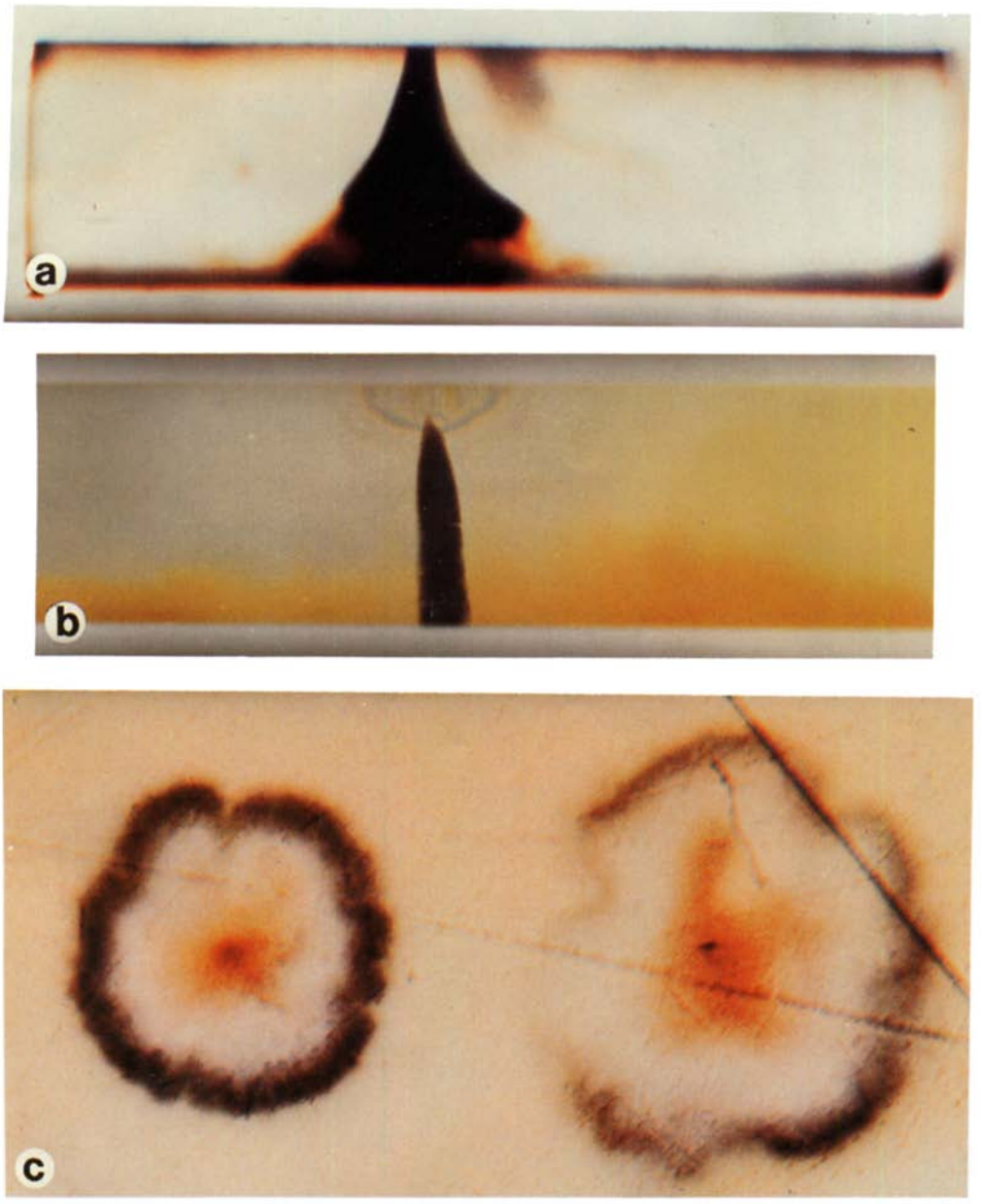

FIG. 2. Electrolytic coloration effects in doped MgO single crystals. (a) Cross-sectional view of a manganese-doped sample treated in the apparatus illustrated in Fig. 1 for 2 hr at 1050°C and an applied voltage of 1100 V. The crystal is approximately 2.5 mm thick (i.e., from the top to the bottom surface); (b) cross-sectional view of an Fe-doped MgO crystal treated for 42 hr at 1050°C and an applied voltage of 1800 V. The crystal is approximately 2.5 mm thick; and (c) top view (i.e., along the long direction of the point contact wire) of a vanadium-doped MgO single crystal treated for 3 hr at 1050°C and 1400 V. The coloration takes the form of concentric cylinders and the different regions result from the variation in redox conditions as a function of distance from the cathode. The diameter of the dark outer ring on the left-hand side is about 3.0 mm.

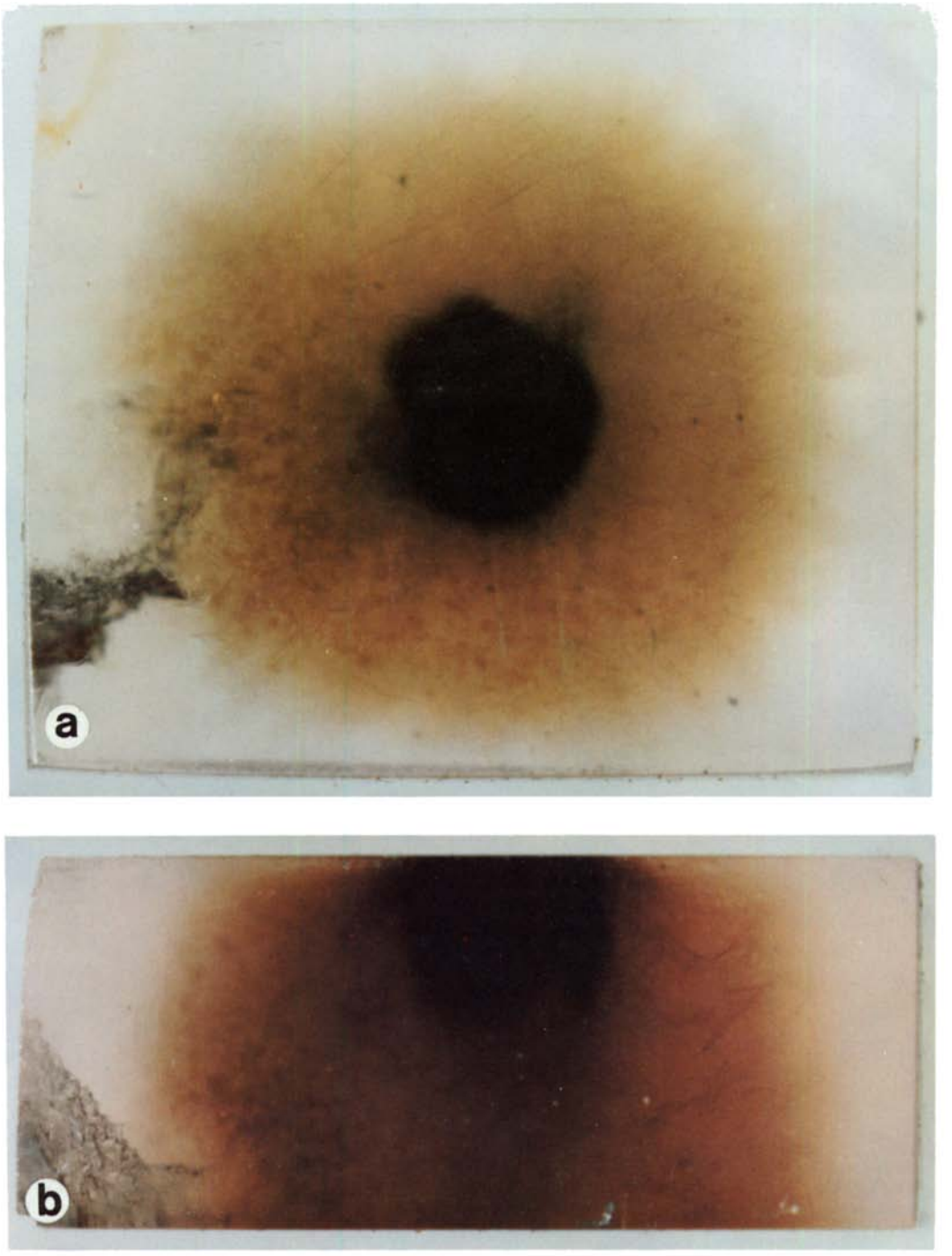

FIG. 3. Electrolytic coloration effects in a single crystal of cobalt-doped MgO. (a) Top view of a sample treated for 2 hr at 1050°C and an applied voltage of 1500 V; (b) cross-sectional view of the same sample showing the structure of the complex coloration formed in this material.

pletely reliable in all cases. The qualitative features of the optical measurements, however, clearly establish that the dark coloration is due, either totally or in large part, to metallic precipitates of electrolytically reduced impurities. The existence of small particles in the treated crystals is immediately revealed by the observation of light scattering at large angles. The magnetic circular dichroism (MCD) of the areas of electrically induced coloration is particularly revealing. Figure 4 shows the MCD and optical absorption of an electrolytically colored Norton sample that was not intentionally doped but which contained iron as well as nickel as the predominant impurities.

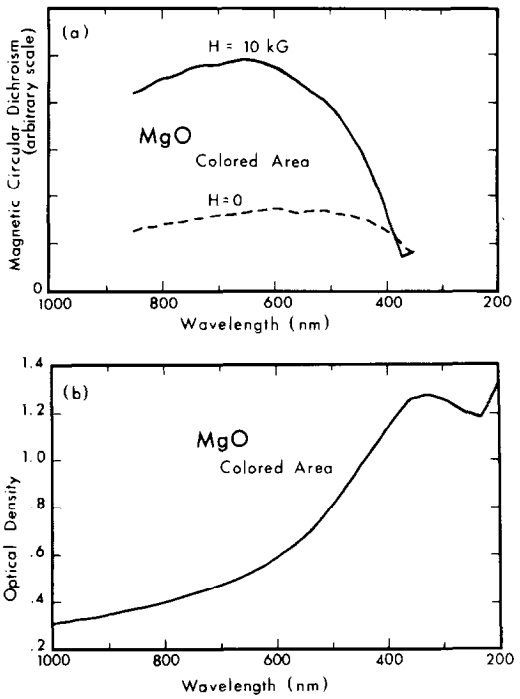

FIG. 4. Spectra of an electrolytically colored Norton MgO crystal. (a) MCD spectrum as a function of wavelength at a magnetic field of 10 kG and the remanent MCD spectrum after the external magnetic field is removed; (b) plot of optical density vs wavelength for the same crystal. EPR observations showed that this specimen contained a significant concentration (~0.1 at.%) of Ni as an impurity. This observation was also confirmed by optical emission spectroscopy.

The significant results are, first, that a very large MCD (as much as 10% of the absorption) is induced by a 10-kG magnetic field at room temperature and, second, that a substantial portion of the MCD persists after the external magnetic field is removed. On the basis of these results, it is concluded that much of the coloration is contributed by ferromagnetic particles. The conclusion that ferromagnetic particles had formed in the crystal was verified by simply observing that small pieces of the colored crystals were attracted to a permanent magnetron magnet. Figure 5 shows magneto-optical hysteresis loops that establish even more clearly the connection between a ferromagnetic impurity and electrolytically induced coloration. As can be seen from Fig. 5, the hysteresis loops change shape when observed at different wavelengths and even become multiple loops at some wavelengths. These shape changes, which are somewhat similar to those observed for $NiFe_2O_4$ films (*10*), suggest that the coloration originates from particles that vary in size and/or composition.

Additional evidence that the coloration is produced by electrolytic reduction of dissolved impurities is provided by the MCD measurements. As a test of this model, an MgO crystal doped with nickel was reduced by heating in a hydrogen gas atmosphere for 2 days at 1050°C. The treatment produced a darkly colored crystal which, when the crystal was cleaved, still revealed the original lighter green color due to unreduced Ni^{2+} in the central portion. The MCD spectra of this crystal measured before and after the hydrogen reduction are shown in Fig. 6 along with the results for a different piece of the same crystal that was colored by the application of an electric field for 2 hr at 1050°C. From these spectra, it is concluded that the dark coloration produced by an electric field is the result of the electrolytic reduction of impurities. It is clear that a strong electric field produces the same ef-

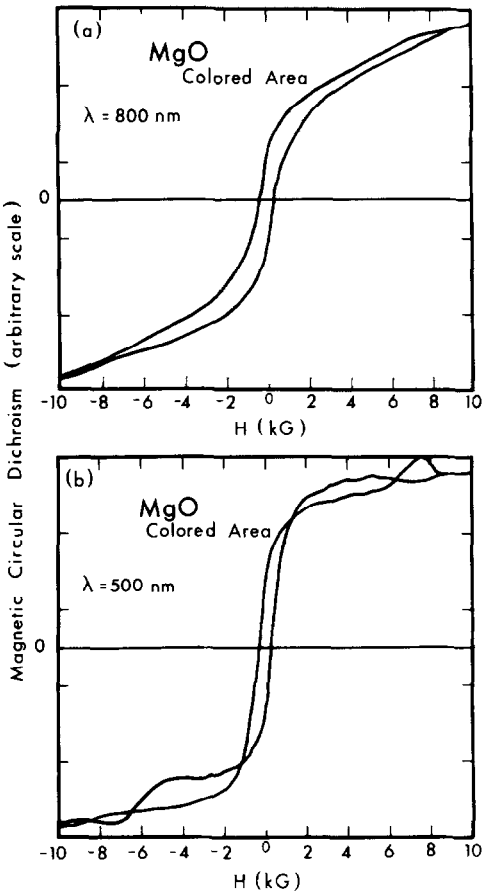

FIG. 5. Spectra of an electrolytically colored Norton MgO crystal. MCD spectra as a function of applied magnetic field. Top and bottom traces show measurements made at wavelengths of 800 and 500 nm, respectively. Hysteresis effects that vary with the wavelength are clearly in evidence.

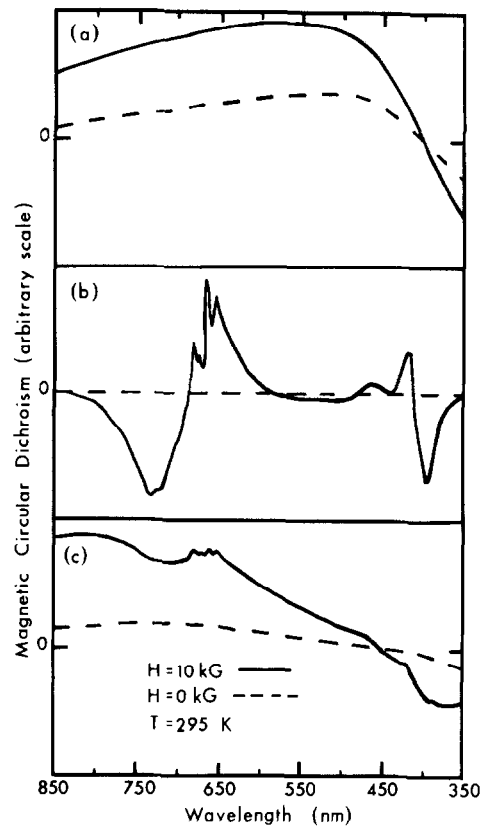

FIG. 6. MCD spectra of an ORNL grown crystal of MgO doped with Ni. (a) MCD spectrum of a colored area produced by applying an electric field on the crystal at 1050°C for 2 hr; (b) spectrum attributable to Ni^{2+} in a clear area; (c) spectrum of a portion of the crystal that was darkened by reduction in H_2 at 1050°C for 48 hr. The spectra represented by dashed curves were measured at zero magnetic field after the spectra represented by the solid curves were measured at 10 kG.

fect as hydrogen reduction at a comparable temperature but that the electrolytic effects occur much more rapidly. Davidge (*11*) has observed the production of a similar dark coloration in Fe-doped MgO crystals that were heated in hydrogen; and, from X-ray studies, he has identified the coloration as due to small precipitates of *bcc* iron. Hence, it is readily concluded that the dark streaks that accompany the electrical breakdown of MgO are mainly due to metallic precipitates produced by the electrolytic reduction of impurities.

The magneto-optical studies also provide evidence pertaining to the size and composition of the metallic precipitates. MCD spectra of samples that were rapidly cooled from 1050°C are shifted slightly in energy in comparison with the spectra of samples that are cooled slowly. Additionally, the spectra from rapidly cooled samples are characterized by a smaller degree of magnetic hysteresis (see Fig. 7) relative to slowly cooled specimens. These effects are attributed to a "ripening" of the precipitates that occurs during the slow cooling.

The smaller particles that result from rapid cooling of the crystal are relatively less ferromagnetic and more superparamagnetic than are the larger particles produced by slow cooling. The MCD spectra of all electrolytically colored samples exhibited some ferromagnetism, and, hence, the precipitates contain ferromagnetic impurities (presumed to be mostly iron) even when a nonferromagnetic dopant is the predominant impurity. Some of the precipitates are presumed to be alloys of the impurities present in the crystals rather than pure metals.

While the MCD results show that metallic colloids are responsible for all or most of the coloration, an exact interpretation of the MCD spectra is precluded. In more favorable cases, Mie theory (*8*) can supply an interpretation of the light scattering effects arising from small precipitates; and, for some very simple cases, the magneto-optical spectra of colloids have been interpreted in detail (*12*). In the present case, however, uncertainties in the optical spectra arising from the inhomogenity of the electrically induced coloration, together with uncertainties regarding the exact composition, optical constants, and size distributions of the colloids, prohibit a detailed interpretation. Nevertheless, an understanding of both the optical and electrical properties of the dark streaks produced by electrolytic coloration in MgO can be obtained from Maxwell Garnett's theory (*13*) for the dielectric function of a composite of spherical metal inclusions in a dielectric host. According to this theory, an effective complex dielectric function for the composite is given by

$$\tilde{\varepsilon} = \varepsilon^{d}\left[\frac{1 + 2F(\varepsilon^{m} - \varepsilon^{d})/(\varepsilon^{m} + 2\varepsilon^{d})}{1 - F(\varepsilon^{m} - \varepsilon^{d})/(\varepsilon^{m} + 2\varepsilon^{d})}\right] \quad (1)$$

where ε^{d} and ε^{m} refer to the dielectric functions of the dielectric and metal, respectively, and F is the volume fraction of the metal.

Garnett's result is of interest at low frequencies as well as at the higher optical frequencies. At low frequencies, free carrier contributions to the dielectric function predominate, and Maxwell's equation for the conductivity of such a composite (*14*) can be obtained by substituting $-i\sigma/\omega$ for ε. Since the conductivity of the metal is much larger than that of the dielectric, an expansion of Eq. (1) for small F reduces to

$$\tilde{\sigma} \simeq \sigma_{d}(1 + 3F). \quad (2)$$

Hence, the highly conducting metal colloids will have a negligible direct effect on the conductivity of the dark streak.

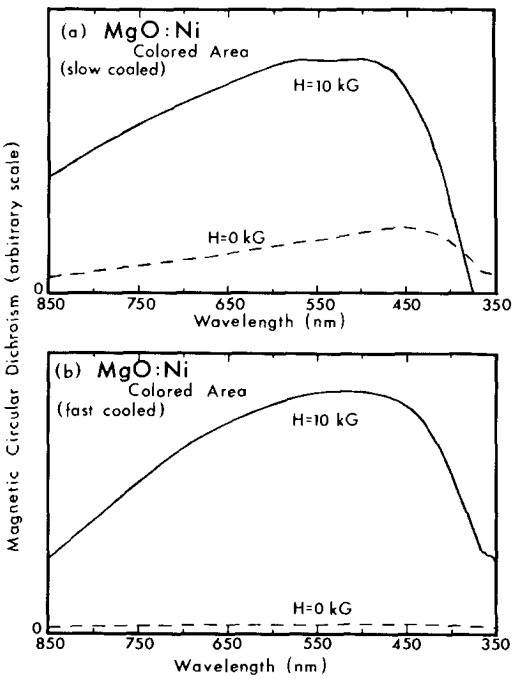

FIG. 7. Spectra of electrolytically colored ORNL-grown MgO : Ni crystals. (a) MCD spectra as a function of wavelength for a crystal that was slowly cooled from 1050°C; (b) MCD spectra of a similar crystal that was rapidly cooled from 1050°C to room temperature. The spectra measured at 10 kG are similar, but the remanent spectra measured at zero magnetic field are different. The slowly cooled crystal is relatively more ferromagnetic, while the rapidly cooled crystal exhibits no hysteresis and is more superparamagnetic.

At optical frequencies, Eq. (1) reveals that resonance effects are possible if $\varepsilon^m \sim -2\varepsilon^d$. This resonance condition is often met for metal/insulator composites because the real part of the metal dielectric function increases smoothly from a large negative value at low frequency to a positive value at optical frequencies, whereas the insulator dielectric function is positive and nearly constant in the same frequency range.

If an effective optical absorption coefficient (α) is computed to lowest order in F from Eq. (1), the first term of the Mie theory (*8*) series is obtained:

$$\alpha = \left[\frac{18\pi F}{\lambda}\right]\left\{\frac{(\varepsilon_1^d)^{3/2}\varepsilon_2^m}{(\varepsilon_1^m + 2\varepsilon_1^d)^2 + (\varepsilon_2^m)^2}\right\} \quad (3)$$

where the subscripts 1 and 2 refer to the real and imaginary parts of the complex dielectric functions, respectively, and λ is the optical wavelength. Equation (3) provides an interpretation of the dark coloration observed in electrically colored MgO. An absorption resonance is predicted in the visible spectrum if $\varepsilon_1^m = -2\varepsilon_1^d$ in this region, and the iron-group transition metals satisfy this requirement. (For example, ε_1^m for both Cu and Ni is ~ -6 at near 2.5 eV (*15*) and $\varepsilon_1^d \sim 3$ for MgO.) As a result of the absorption resonance, a very dark coloration can arise from low volume fractions of the metal. Figure 4b shows the experimental absorption spectrum of a typical dark streak. The position of this absorption between 2.0 and 4.0 eV (i.e., ~600 to 300 nm) agrees well with the theoretical predictions of an absorption resonance in this region, and the spectrum is similar to that reported by Craighead *et al.* (*16*) for an MgO : Ni composite.

The description of the optical absorption given by Eq. (3) is approximate for several reasons: The results of Davidge (*11*) suggest that the particles are not necessarily spherical and a distribution of particle sizes is expected. Particle size effects can modify optical constants and broaden the resonance absorption. The equation is only valid for particle sizes smaller than the optical wavelength. Larger particles yield a broader absorption spectrum that is described by higher-order terms of a Mie series.

Since larger particles become efficient light scatterers, the particle size distribution in the streaks may be investigated by measuring the angular distribution of scattered laser radiation. Two treated MgO samples were studied by means of an imaging goniometer system with which a specific region of the crystal could be examined by the phototube detector. In this way, scattered light from different regions within an individual dark streak could be measured. The resulting angular distributions can be qualitatively interpreted graphically from plots (*17*) of $\log[I(\Theta)\ \sin^2\Theta/2)]$ vs $\log(\sin\Theta/2)$. Such graphs, called modified Sloan Plots, show peaks from which the dominant particle sizes may be read directly, and widths from which particle size distributions may be inferred. These qualitative results depend only on the *form* of $I(\Theta)$, not on absolute intensities, and are nearly independent of indices of refraction and particle shapes. They provide a valuable guide for interactive computer fitting by which the angular distributions are deconvoluted. For the present samples, the particle sizes are all smaller than ~2 μm and the major part of the angular distribution of the scattered light is therefore contained in the forward lobe region (i.e., that part in which the initial drop in scattering intensity vs angle takes place).

Approximate computer fitting procedures for the angular dependence of the scattered light (*18, 19*) yield size distributions that are in agreement with those indicated on the Sloan Plots. Least squares regression is used to fit the measured angular distributions to an array of trial size distributions. These are obtained from a series of

size parameters chosen to span the range of sizes in the sample. This basis set of angular distributions then is used to produce a size distribution which minimizes deviations from the measured angular distribution. Such procedures are useful when the angular distribution consists entirely of forward lobe information or is so polydisperse as to have no resolved secondary lobe structure. Figure 8 shows a calculated fit to the experimental angular distribution, and Fig. 9 shows the corresponding size distribution derived from the results illustrated in Fig. 8 for a representative region of a dark streak. Small angle scattering from surfaces and internal cracks limited the upper range of particle sizes which could be measured. In the samples examined, there are parts of the streak in which the large angle scattering ($\Theta > 90°$) is quite isotropic, suggesting that there is a large population of particles whose diameter is less than 0.1 μm. The observed size distributions vary significantly depending on the position being examined in the streak. An example of the size distribution from a part of a streak containing small particles is shown in Fig. 9. This region contains particles of diameter ~0.3 to 0.7 μm and a smaller fraction of particles ~1.5 μm in diameter. The results

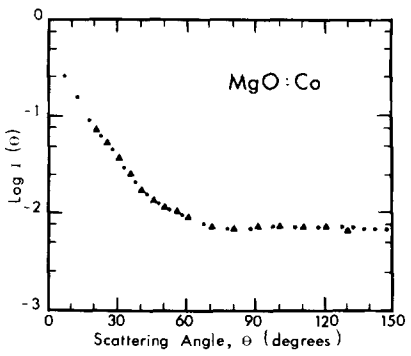

FIG. 8. Plot of relative intensity $I(\Theta)$ of scattered light vs the scattering angle Θ. The measured values are denoted by triangles and the dots represent the computer fit. The scattered light was from a dark streak produced by electrolytic coloration in cobalt-doped MgO.

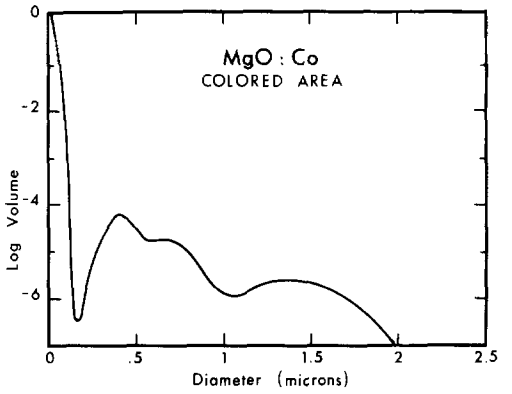

FIG. 9. Plot of the relative precipitated volume vs particle diameter, which results from the computer fit shown in Fig. 8.

indicate that the sizes and distributions are determined by formation conditions and will probably vary from sample to sample as well. Because particle densities within the streaks are generally quite high, good scattering measurements could be made only on specially prepared samples in which the particle formation was intentionally arrested. These specially prepared samples had particle densities sufficiently low to minimize multiple scattering effects.

V. Magnetic Resonance Studies

Magnetic resonance studies were initially performed using the two Norton samples supplied by Sonder *et al.* (*1*). Differences were observed between the resonance spectra of the clear and dark portions of the crystals. Broad EPR signals were observed in the dark portions of the samples that were not found when clear regions of the crystal were examined. In Fig. 10, the spectrum of a dark section of the crystal is shown with the magnetic field along a crystal [100] crystallographic axis. The sharp lines in the spectrum are due to isolated Mn^{2+}, Fe^{3+}, and Cr^{3+} impurities. These spectra were also seen in a clear piece of the same crystal. A low-field broad signal associated with the dark areas of the

crystal was slightly anisotropic with respect to the applied magnetic field orientation and changed shape as the magnetic field was rotated away from the crystal [100] axis (see Fig. 10) towards the [110] axis. Another broad line which exhibited increased anisotropy in both its magnetic field position and linewidth appears in Fig. 10 which can be seen with **H**||[111] and **H**||[110] and in Fig. 11 with **H** at various angles in the (110) plane. This signal, whose g value varied from $g \simeq 0.5$ in the [100] direction (with a linewidth exceeding 1000 G) to $g \simeq 2.0$ in the [111] direction (with a much narrower linewidth of ~250 G), was noteworthy in that the high field extreme occurred only when the applied magnetic field lay along

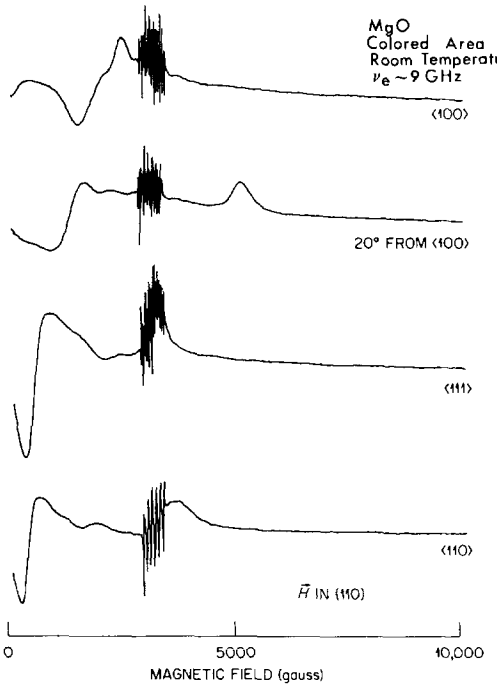

FIG. 10. The magnetic resonance spectrum of an electrolytically colored Norton MgO crystal. The sharp lines are due to Mn^{2+}, Fe^{3+}, and Cr^{3+} isolated impurities, which were also seen in a clear piece of the same crystal. Broad lines which are anisotropic in both position and linewidth may be seen in these traces with the magnetic field **H** in the (110) plane and oriented along the ⟨100⟩ direction, 20° from the ⟨100⟩ direction, the ⟨111⟩ direction, and the ⟨110⟩ direction.

the long dimension of the streak that was parallel to a [100] crystal axis and was not present when the field was applied along the two other [100] directions. That is, the signal did not follow the full crystallographic symmetry and three equivalent signals (i.e., one for each ⟨100⟩ axis) were not observed. The intensity of the broad signals was found to be very temperature dependent. At room temperature, the intensity of the broad signals was much larger than at 77 K and the signals could not be observed at all at $T = 4.2$ K.

As noted in Section III, MgO crystals doped with each element in the complete $3d$ series (with the exception of Sc) were colored electrolytically and sudden increases in the conductivity were observed in every case. The EPR spectrum obtained from a dark portion of a crystal was compared to that obtained from a clear portion of the same crystal and no differences were observed for samples doped with Ti, V, Mn, and Cu. Additional broad EPR lines were observed, however, in the colored region of treated MgO : Ni, Fe, Cr, Co specimens.

VI. Compositional Studies

Analyses of the composition of the dark streaks were carried out by means of secondary ion mass spectrometry (SIMS) and X-ray fluorescence spectroscopy (XFS). The SIMS analysis disclosed that the formation of a dark streak did not produce a significant long-range gradient in the impurity concentration. Figure 12 shows the results obtained using an ORNL Ni-doped MgO crystal which had been subjected to a 24-hr treatment at $T = 1050$°C and a voltage of 1500 V in the apparatus shown schematically in Fig. 1a. It can be seen that the impurity concentration obtained in the electrolytically colored region of the crystal (shown at the top of the Fig. 12) is identical with that obtained in a neighboring clear re-

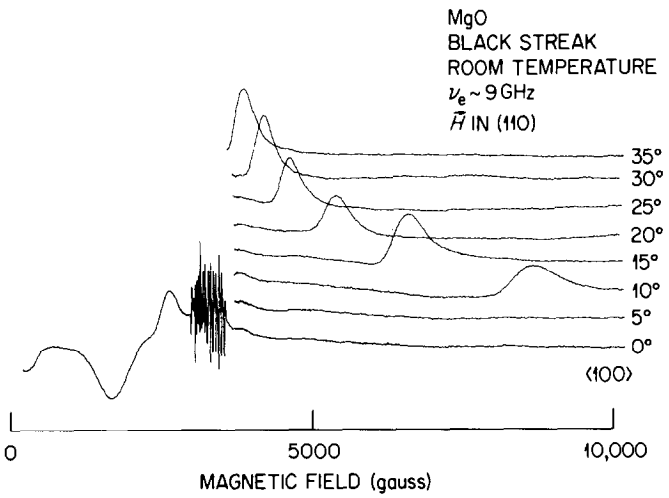

FIG. 11. Angular variation of the magnetic resonance absorption observed in an electrolytically colored Norton MgO crystal. The spectrum is shown for the magnetic field **H** oriented at various angles in the (110) plane.

gion of the crystal (shown at the bottom of Fig. 12). Thus, it appears that there is no significant impurity migration over large distances and that the streaks are produced by local chemical changes which occur without corresponding compositional changes on a macroscopic scale. The XFS, however, does show some alloying of impurities with the electrodes. This observation is also corroborated by the fact that the cathode often physically welded to the samples during the electrolytic treatment.

VII. Summary

An electrolytic reduction technique, in which a platinum point-contact cathode was used, has been employed in reproducing the localized coloration effects previously observed (*1*) as an unidentified artifact in measurements of the electrical properties of MgO single crystals at elevated (~1000°C) temperatures. In the simple electrolytic treatment system employed in the present investigations, direct, real time observations of the initiation and development of electrolytic coloration could

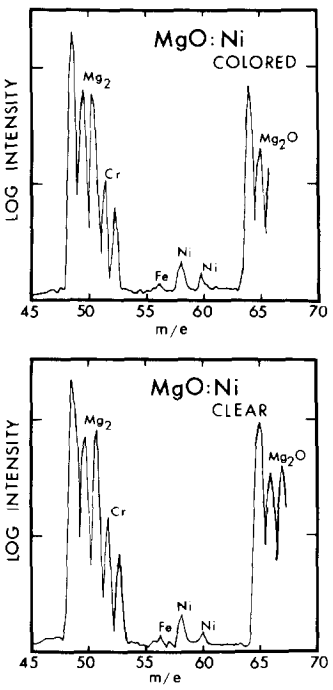

FIG. 12. Plot of log of the intensity (concentration) vs *m/e* obtained by secondary ion mass spectroscopy (SIMS). The top figure shows results for an ORNL MgO : Ni crystal which was electrolytically colored and the bottom figure shows that essentially the same elemental concentrations are found in an adjacent clear area of the crystal.

be made. Since *in situ* changes of the position of the point-contact cathode relative to the face of the MgO single crystal were feasible, it was possible to establish that the areas of electrolytic coloration coincided with the regions of high electrical conductivity that are responsible for catastrophic failure in the electrical insulating properties of MgO at elevated temperatures. Additionally, direct observations of the initiation of the coloration prove that the process begins at the cathode and gradually extends across the MgO single crystal until it eventually reaches the anode. Coloration effects were produced in MgO crystals doped with every member of the iron group transition series with the exception of scandium. Interesting differences in the tendency toward electrical breakdown were observed for different impurities. Electrolytic coloration was not observed in the purest MgO crystals, but it was still possible to induce thermal-electrical breakdown in these specimens.

A number of characterization techniques were used to establish that the observed electrolytic coloration arises primarily from the formation of metallic precipitates that result from the reduction of impurities. Similar coloration effects were induced in intentionally doped MgO single crystals by means of standard reduction techniques such as heating the samples in a hydrogen atmosphere. MCD examinations indicated that the metallic precipitates were strongly ferromagnetic in the case of Fe or Ni doped MgO and only slightly ferromagnetic in crystals intentionally doped with other elements. In such cases, this weak ferromagnetism is attributed to ferromagnetic impurities that are present at lower levels than the intentionally added dopant.

As noted previously, the technique of electrolytic coloration has been applied to the alkali halides for many years (*6, 20*). Accordingly, it is somewhat surprising that so little has been done by way of extending the technique to altering the properties of oxides such as MgO. As can be seen in Figs. 2a,b,c and Fig. 3, the technique represents a simple method for producing significant solid state chemical alterations in the properties of refractory oxides.

References

1. E. Sonder, K. Kelton, J. C. Pigg, and R. A. Weeks, *J. Appl. Phys.* **49,** 5971 (1978).
2. J. Narayan, R. A. Weeks, and E. Sonder, *J. Appl. Phys.* **49,** 5977 (1978).
3. L. A. Boatner, F. A. Modine, M. M. Abraham, and W. H. Christie, *Bull. Amer. Phys. Soc.* **24,** 413 (1979).
4. M. M. Abraham, L. A. Boatner, and F. A. Modine, *Bull. Amer. Phys. Soc.* **24,** 413 (1979).
5. F. A. Modine, L. A. Boatner, M. M. Abraham, W. P. Unruh, and R. Bunch, *Bull. Amer. Phys. Soc.* **24,** 413 (1979).
6. J. H. Schulman and W. D. Compton, "Color Centers in Solids," International Series of Monographs on Solid State Physics, Vol. II pp. 34–41, 91–94, 256–273, Pergamon, Oxford (1962).
7. M. M. Abraham, C. T. Butler, and Y. Chen, *J. Chem. Phys.* **55,** 3752 (1971).
8. G. Mie, *Ann. Phys.* **25,** 377 (1908); see also A. E. Hughes and S. C. Jain, *Adv. Phys.* **28,** 717 (1979), and references therein.
9. F. A. Modine, Y. Chen, and R. W. Major, and T. M. Wilson, *Phys. Rev. B* **14,** 1739 (1976).
10. R. L. Coren and M. H. Francombe, *J. Phys. Colloq. Orsay Fr.* **25,** 233 (1964).
11. R. W. Davidge, *J. Mater. Sci.* **2,** 339 (1967).
12. F. A. Modine and V. M. Orera, *Phys. Rev. B* **24,** 1159 (1981).
13. J. C. Maxwell Garnett, *Philos. Trans. R. Soc. London* **203,** 385 (1904); **205,** 237 (1906); J. P. Marton and J. R. Lemon, *Phys. Rev. B* **4,** 271 (1971); *J. Appl. Phys.* **44,,** 3953 (1973).
14. J. C. Maxwell, "Treatise on Electricity and Magnetism," Vol. I, 3rd ed., Clarendon, London (1892).
15. H. Ehrenreich, H. R. Philipp, and D. J. Olechna, *Phys. Rev.* **131,** 2469 (1963).
16. H. G. Craighead, R. Bartynski, R. A. Buhrman, L. Wojcik, and A. J. Sievers, *Sol. Energy Mater.* **1,** 105 (1979).
17. P. J. Livesly and F. W. Billmeyer, *J. Colloid Sci.* **30,** 447 (1969).
18. R. M. Bunch, Thesis, University of Kansas (1981) (University Microfilms, Ann Arbor, Mich.).
19. T. W. Alger, *Appl. Opt.* **19,** 2428 (1980).
20. R. W. Pohl, *Proc. Phys. Soc.* **49,** extra part (1937), Physics Society of London.